PERFORMANCE COMPARISON OF DIFFERENT SYSTEM IDENTIFICATION ALGORITHMS FOR FACET AND ATF2

J. Pfingstner*, A. Latina, D. Schulte, CERN, Geneva, Switzerland

Abstract

Good system knowledge is an essential ingredient for the operation of modern accelerator facilities. For example, beam-based alignment algorithms and orbit feedbacks rely strongly on a precise measurement of the orbit response matrix. The quality of the measurement of this matrix can be improved over time by statistically combining the effects of small system excitations with the help of system identification algorithms. These small excitations can be applied in a parasitic mode without stopping the accelerator operation (on-line). In this work, different system identification algorithms are used in simulation studies for the response matrix measurement at ATF2. The results for ATF2 are finally compared with the results for FACET, latter originating from an earlier work.

INTRODUCTION

Since modern particle accelerators are becoming increasingly more complex, automated techniques for beam-based alignment, beam steering, and diagnostics and error detection tools become more and more important. In very large machine, the accelerator operation without automated strategies would be even impossible, since the too large number of components would not allow a machine tuning by hand. Most of the mentioned algorithms rely on precise system knowledge in form of the orbit response matrix $\boldsymbol{R}$.

In this work we apply techniques from the field of system identification to measure the orbit response matrix in a parasitic way without stopping the usual accelerator operation (on-line). Therefore, small beam oscillations are introduced by the actuation of kicker magnets. The resulting beam oscillations are measured by the beam position monitors (BPMs) distributed along the beam line. These measurements together with the known actuations of the kicker magnets can be used by system identification algorithms to estimate the orbit response matrix over time. These algorithms combine the data in order to statistically reduce the BPM noise content in the measurements.

Different system identification schemes for FACET [1] have been already studied earlier [2] and in the meanwhile have been fruitfully deployed for the dispersion free steering correction at this machine. Another important test facility that has many important applications that could profit strongly from very precise system knowledge is ATF2 [3]. Examples for such applications are beam trajectory correction systems [4] and experiments that intent to reconstruct the beam motion form measured ground motion [5]. Therefore, in this work several different system identification algorithms are tested via simulations studies with the tracking code PLACET [7] for ATF2. Finally, the differences between FACET and ATF2 with respect to the application of system identification techniques are discussed.

EXCITATION SCHEMES AND IDENTIFICATIONS ALGORITHMS

The beam excitation schemes used for the system identification at ATF2 are adjusted to the main goal of ATF2, which is to produce very small beam sizes, e.g. 40 nm in the vertical direction at the interaction point (IP). Therefore, the objective of the excitation is to increase the projected beam size of several bunches (including beam offset jitter) by only a small value. However, it would not be a robust strategy to scale the excitation of each corrector to create a certain given growth of the projected beam size. The reason is that, due to the design of the ATF2 beam line and the beam structure itself, there is hardly any beam size growth linked to beam oscillations along the beam line, but only an increase of the beam offset at the IP. If the phase advance from the kick position to the IP is now close to a multiple of π, hardly any beam offset can be observed at the IP, even though there could be already too large oscillations along the beam line with respect to the given aperture limitations. Instead a different strategy is followed. The kicker actuation $u(i)$ of the ith kicker is calculated to produced a wanted relative multi-pulse emittance growth $\Delta\epsilon_r = (\epsilon_m - \epsilon_0)/\epsilon_0$, where ϵ_0 is the nominal single-pulse emittance and ϵ_m the multi-pulse emittance at the IP. Such an actuation is given by

$$u(i) = \sqrt{\frac{\Delta\epsilon_r}{f_\epsilon(i)}}, \tag{1}$$

where the $f_\epsilon(i)$ are scaling factors determined via simulation for each kicker magnet. To convert the wanted relative growth of the projected beam size $\Delta\sigma_r = (\sigma_m - \sigma_0)/\sigma_0$, where σ_0 is the nominal beam size at the IP and σ_m the multi-pulse beam size at the IP, the following relation is used

$$\begin{aligned} \frac{\sigma_m}{\sigma_s} &= \sqrt{\frac{\epsilon_m}{\epsilon_s}} \\ 1 + \Delta\sigma_r &= \sqrt{1 + \Delta\epsilon_r} \\ \Rightarrow \Delta\epsilon_r &= (1 + \Delta\sigma_r)^2 - 1. \end{aligned} \tag{2}$$

There are two type of excitations applied. In the first, each kicker magnet is used one after each other to induce beam oscillations. This excitation is therefore called orthogonal excitation. In the second type of excitation, each kicker is

* juergen.pfingstner@cern.ch

ISBN 978-3-95450-122-9

actuated at the same time in a random fashion. Since the emittance growth of different induced kicks adds linearly, the overall specified emittance growth $\Delta\epsilon_r$ has to be divided in case of the random excitation by the number of used kickers $N = 13$ and then used in Eq. (1) to calculate the kicker actuations.

The used system identification algorithms and in general the system identification metrology will be only briefly introduced in the following. A more detailed discussion can be found in [2]. Since the measurements of an individual BPM is not dependent on the measurements of other BPMs, each row of the orbit response matrix can be identified separately. The big identification problem can therefore be split into several smaller identification problems, one for each of the 55 BPMs of ATF2. The system to be identified for one BPM has the form

$$y_k = [\boldsymbol{r}^T\, d] \begin{bmatrix} \boldsymbol{u}_k \\ 1 \end{bmatrix} + n_k, \qquad (3)$$

where y_k is the BPM reading at time step k, $\boldsymbol{u}_k$ is the vector of all kicker actuations, $\boldsymbol{r}^T$ is the row of the orbit response matrix $\boldsymbol{R}$ that corresponds to the BPM, d is the reference orbit without excitation and n_k is BPM noise. Given this system form, all tested identification algorithms can be written in the form

$$\begin{aligned} \hat{\boldsymbol{\theta}}_k &= \hat{\boldsymbol{\theta}}_{k-1} + \boldsymbol{K}_k e_k \quad \text{with} \qquad (4) \\ \boldsymbol{e}_k &= y_k - \hat{\boldsymbol{\theta}}_{k-1}^T \boldsymbol{\phi}_k, \\ \hat{\boldsymbol{\theta}}_{k-1}^T &= \left[\hat{\boldsymbol{r}}_k^T,\, \hat{d}_k\right] \quad \text{and} \quad \boldsymbol{\phi}_k^T = \left[\boldsymbol{u}_k^T,\, 1\right], \end{aligned}$$

where the hat-index distinguishes the estimated parameters $\hat{\boldsymbol{\theta}}_k$ from the real $\boldsymbol{\theta}_k$. The recursive least squares (RLS), the stochastic approximation (SA), and the least mean squares (LMS) algorithm only differ in the way the update matrix $\boldsymbol{K}_k$ is calculated. For the RLS algorithm this matrix is given by

$$\begin{aligned} \boldsymbol{K}_k &= \boldsymbol{P}_{k-1}\boldsymbol{\phi}_k \left(1 - \boldsymbol{\phi}_k^T \boldsymbol{P}_{k-1}\boldsymbol{\phi}_k\right)^{-1} \qquad (5) \\ \boldsymbol{P}_k &= \left(\boldsymbol{I} - \boldsymbol{K}_k \boldsymbol{\phi}_k^T\right) \boldsymbol{P}_{k-1}, \end{aligned}$$

for the SA algorithm by

$$\boldsymbol{K}_k = \frac{1}{\sum_{n=1}^{k} \boldsymbol{\phi}_n^T \boldsymbol{\phi}_n} \boldsymbol{\phi}_k, \qquad (6)$$

and for the LMS algorithm by

$$\boldsymbol{K}_k = \gamma \boldsymbol{\phi}_k, \qquad (7)$$

where γ is a constant update parameter. Detailed discussions about the derivation and the properties of these algorithms can be found in [6]. It should be mentioned however, that the RLS algorithm is optimal in a quadratic sense for the identification of the system Eq. (3). The LMS and the SA algorithms are simplifications of the computationally more expensive RLS algorithm.

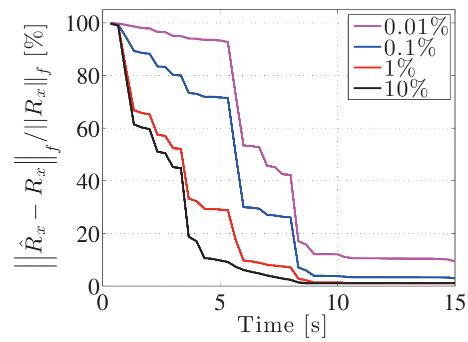

Figure 1: Relative quadratic error of the estimated orbit response matrix $\hat{\boldsymbol{R}}_x$ compared to the real orbit response matrix $\boldsymbol{R}_x$ in the horizontal direction measured in the Frobenius norm. The matrix $\hat{\boldsymbol{R}}_x$ was estimated with the RLS algorithm with orthogonal excitation. The curves correspond to different excitations yielding the indicated values of projected beam size growth.

SIMULATIONS RESULTS FOR ATF2 AND COMPARISON TO FACET RESULTS

The before mentioned excitation schemes and identification algorithms have been tested via simulation in PLACET [7]. The results show that due to the induced beam oscillations by the system identification, the single-pulse emittance of the beam at the IP is hardly increased. Basically all increase of the multi-pulse emittance is due to the induced jitter. This is very different compared to FACET, where the strong wake fields, the high beam energy spread and the long linac cause strong single-pulse emittance growth. Another advantage at ATF2 is that the BPM system has a much better resolution than at FACET, which suggests that the estimation times will be shorter at ATF2. Also due to the smaller number of kicker magnets at ATF2 (13 instead of 67), a shorter identification time by about an additional factor of 5 has to be expected.

All these apparent advantages at ATF2 are reflected in the identification results. In Fig. 1 and Fig. 2 the results of the RLS algorithm with orthogonal excitation are shown. The necessary time to estimate the orbit response matrix to better than 5% is for both cases around 10 s. This can be achieved with and induced projected beam size growth of only 1%. In more detail, after 10 s the error is 1.5% and 3% in horizontal and vertical direction. It seems to be not very useful to use stronger excitations. The horizontal direction can be identified more accurately, since the excitation for the same projected beam size growth is larger by about a factor 2 compared to the vertical direction. However, the estimation is very fast in both directions, since the signal to noise ratio of the measurements is high. Only after about 8 s, when the matrix is updated for the first time fully, the noise averaging is starting. At this time the matrix is already known to a high precision. It is interesting to see however that such a fast measurement is possible

ISBN 978-3-95450-122-9

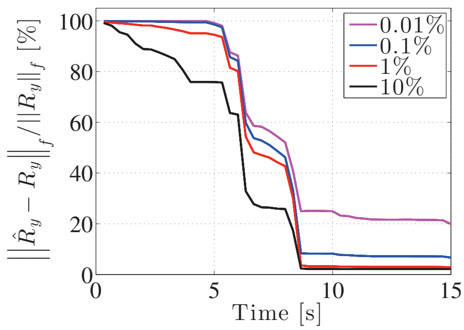

Figure 2: Relative quadratic error of the estimated orbit response matrix $\hat{\boldsymbol{R}}_y$ compared to the real orbit response matrix $\boldsymbol{R}_y$ in the vertical direction measured in the Frobenius norm. The matrix $\hat{\boldsymbol{R}}_y$ was estimated with the RLS algorithm with orthogonal excitation. TThe curves correspond to different excitations yielding the indicated values of projected beam size growth.

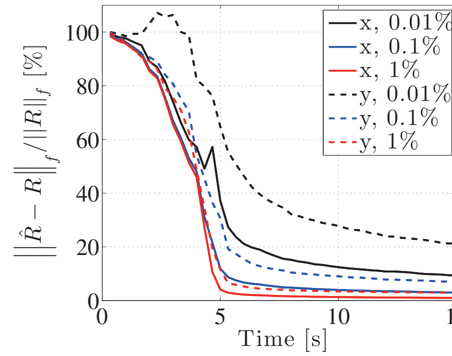

Figure 3: Relative quadratic error of the estimated orbit response matrix $\hat{\boldsymbol{R}}$ compared to the real orbit response matrix $\boldsymbol{R}$ in the vertical and horizontal direction measured in the Frobenius norm. The matrix $\hat{\boldsymbol{R}}$ was estimated with the RLS algorithm with random excitation. The curves correspond to different excitations yielding the indicated values of projected beam size growth.

basically fully parasitic with negligible growth of the projected emittance at ATF2. This is in contrast to the FACET linac, where the identification in a parasitic mode is hardly possible and also with high induced emittance growth the matrix can only be estimated to the same precision after several minutes to hours.

In Fig. 3 the performance of the RLS algorithm with random excitation in horizontal and vertical direction is shown. Both, the orthogonal and the random excitation show similar performance after about 10 s, but the random excitation identifies the system faster over shorter times. This is due to the reason that with the random excitation all parameters to be estimated are tested from the first excitation on, while the orthogonal excitation, which excites only one kicker magnet at a time, needs about 8 s to excite each kicker magnet in positive and negative direction. Also in this plot it is apparent that the matrix on horizontal direction can be estimated fast than in the vertical direction due to the larger excitation for the same growth of the projected beam size.

Finally, in Fig. 4 it is shown that both, the SA and the LMS algorithm, have a worse performance compared to the RLS algorithm. To achieve estimation precisions of a few per cent, estimation times of several minutes are necessary. For $\gamma > 0.7$, the LMS algorithm gets unstable in this application.

CONCLUSIONS

In this work, different system identification algorithms have been applied to the ATF2 beam line in order to measure the orbit response matrix $\boldsymbol{R}$ parasitically. These simulation results have been compared to similar studies performed for FACET. It has been observed that $\boldsymbol{R}$ can be significantly easier estimated at ATF2 than at FACET. Even with only an induced projected beam size growth of 1% at the IP, $\boldsymbol{R}$ can be measured to an precision of about 3% within 10 s in horizontal and vertical direction.

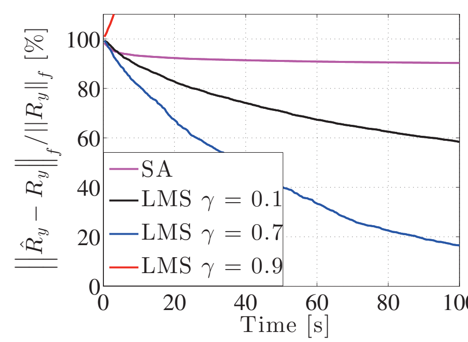

Figure 4: Relative quadratic error of the estimated orbit response matrix $\hat{\boldsymbol{R}}$ compared to the real orbit response matrix $\boldsymbol{R}$ in the vertical direction measured in the Frobenius norm. The matrix $\hat{\boldsymbol{R}}$ was estimated with the SA algorithm and the LMS algorithm for different values of γ, always with random excitation. The excitation has been adjusted such that projected beam size growth is 10%.

REFERENCES

[1] C.I. Clarke et al., In Proc. of IPAC11, WEOAB02, 2011.

[2] J. Pfingstner et al., CERN report, CLIC-Note-946, 2012.

[3] ATF2 Group, ATF2 Proposal, KEK Report 2005-2, CERN-AB-2005-035, 2006.

[4] D.R. Bett et al., In Proc. of IPAC12, WEPPP068, 2012.

[5] Y. Renier et al., In Proc. of IPAC12, TUPPR060, 2012.

[6] K. J. Åström and B. Wittenmark, *Adaptive Control*, Dover Publications, Inc., 2008, ISBN: 0-486-46278-1.

[7] D. Schulte et al., The Tracking code PLACET, https://savannah.cern.ch/ projects/placet, CERN.

ISBN 978-3-95450-122-9